Naval Research Laboratory
Washington, DC 20375-5320

NRL/5708/MR—2022/1

Case-Study Estimation of Dielectric Response Functions for NIR-SWIR Absorbing Dyes by Inverse Analysis of Diffuse Reflectance

RACHEL VIGER, PA

SCOTT A. RAMSEY

TROY MAYO

Signature Technology Office
Tactical Electronic Warfare Division

SAMUEL G. LAMBRAKOS

Computational Multiphysics Systems
Material Science and Technology Division

May 24, 2022

REPORT DOCUMENTATION PAGE

Form Approved
OMB No. 0704-0188

1. REPORT DATE *(DD-MM-YYYY)*	**2. REPORT TYPE**	**3. DATES COVERED** *(From - To)*
24-05-2022	NRL Memorandum Report	

4. TITLE AND SUBTITLE

Case-Study Estimation of Dielectric Response Functions for NIR-SWIR Absorbing Dyes by Inverse Analysis of Diffuse Reflectance

5a. CONTRACT NUMBER

5b. GRANT NUMBER

5c. PROGRAM ELEMENT NUMBER

6. AUTHOR(S)

Rachel Viger, PA, Scott A. Ramsey, Troy Mayo, and Samuel G. Lambrakos

5d. PROJECT NUMBER

5e. TASK NUMBER

5f. WORK UNIT NUMBER
7542

7. PERFORMING ORGANIZATION NAME(S) AND ADDRESS(ES)

Naval Research Laboratory
4555 Overlook Avenue, SW
Washington, DC 20375-5320

8. PERFORMING ORGANIZATION REPORT NUMBER

NRL/5708/MR--2022/1

9. SPONSORING / MONITORING AGENCY NAME(S) AND ADDRESS(ES)

US Special Operations Command,
Special Operations Forces Acquisition, Technology, and Logistics
7701 Tampa Point Blvd
MacDill Air Force Base, Florida 33621

10. SPONSOR / MONITOR'S ACRONYM(S)

USSOCOM

11. SPONSOR / MONITOR'S REPORT NUMBER(S)

12. DISTRIBUTION / AVAILABILITY STATEMENT

DISTRIBUTION STATEMENT A: Approved for public release; distribution is unlimited.

13. SUPPLEMENTARY NOTES

14. ABSTRACT

This study describes a Kramers-Kronig analysis of diffuse reflectance from NIR/SWIR-absorbing dyes on cotton-fabric substrates for estimating dielectric response functions. The calculated response functions provide estimates of the dielectric response characteristics. Since the Kramers-Kronig analysis is applied to diffuse reflectance and not to specular reflectance from uniform bulk material surfaces, it is not assumed as an exact determination of the material permittivity functions. However, the estimated response functions can support the construction of approximate effective medium models capable of estimating reflectance from dyed fabrics. A sensitivity analysis is presented that explores the impact of Kramers-Kronig integration-range incompleteness by examining the influence of lower/upper wavelength smoothing and extrapolation techniques.

15. SUBJECT TERMS

Diffuse reflectance
Dyed fabrics
Parametric modeling
Absorption spectra

16. SECURITY CLASSIFICATION OF:			**17. LIMITATION OF ABSTRACT**	**18. NUMBER OF PAGES**	**19a. NAME OF RESPONSIBLE PERSON**
a. REPORT	**b. ABSTRACT**	**c. THIS PAGE**			Rachel Viger
U	U	U	U	27	**19b. TELEPHONE NUMBER** *(include area code)* (202) 279-5272

This page intentionally left blank.

Table of Contents

This page intentionally left blank.

1. Introduction

Diffuse reflection defines a separate regime for the spectroscopic analysis of materials. The physical processes underlying diffuse reflectance are discussed in references [1-6]. Parametric models applied to these analyses include those based formally on reflection from layered systems, i.e., scattering matrix (S-matrix) and Beer-Lambert Law models [7,8], and the Kubelka-Munk theory of diffuse reflectance [9-12].

This study describes a Kramers-Kronig analysis [7] of diffuse reflectance from NIR-SWIR absorbing dyes on cotton-fabric substrates for the estimation of dielectric response functions. The calculated response functions provide dielectric-response characteristics of the dyes and information on the sensitivity of their interactions with substrates. The calculated response functions can support the development of approximate effective-medium models (EMMs) [7] for estimating reflectance from dyed fabrics. Additionally, this study examines the sensitivity of the dielectric-response functions to the Kramers-Kronig spectral integration range. The absorption spectra for the Kramers-Kronig analysis are incomplete in the sense that they do not necessarily reach zero at the lower and upper wavelengths. The impact of this behavior on the dielectric-response functions is examined using lower/upper wavelength smoothing and extrapolation techniques.

2. Background

Effective medium models (EMMs), based on effective medium theory (EMT) [7], are constructed using different types of weighted averages for dielectric response functions, where the specific type of weighted average depends on the composite material surface topology. Depending on the microstructure, the dielectric response functions – even for relatively pure materials – fundamentally represent the averages over ensembles of different intermolecular configurations. The fact that dielectric functions are ensemble averages provides motivation for construction of EMMs using estimated dielectric response functions. These estimated dielectric functions are mesoscopically averaged and approximate quantities that can, in principle, be constructed using generalizations of EMM formulations. An example of such generalization is represented by Eq. (1), for one of many EMMs, i.e.

$$\langle \varepsilon_{eff} \rangle = \frac{\sum_{i=1}^{N} w_i \varepsilon_i}{\sum_{i=1}^{N} w_i} \quad \Longrightarrow \quad \langle \varepsilon_{eff} \rangle = \frac{\sum_{i=1}^{N} w_i \langle \varepsilon_i \rangle}{\sum_{i=1}^{N} w_i}, \qquad (Eq.\ 1)$$

where the dependence of dielectric response on surface topology contributions to reflectance is represented by the weight coefficients w_i, $i = 1, ..., N$. Referring to Eq. (1), the dielectric response functions $\langle \varepsilon_i \rangle$ are assumed *a priori* as being estimates of dielectric response characteristics, including the influence of interactions with substrates and adjacent mesoscopic segments.

Next, constructing EMMs using estimated dielectric functions requires the calculation of approximate dielectric functions suitable for such construction. This involves Kramers-Kronig analysis, which is formulated for the determination of estimated quantities. In principle, this formulation would apply Kramers-Kronig analysis to specular reflectance from uniform bulk-material surfaces, which is an assumed condition for the accurate determination of material permittivity functions. However, in this case the absorbance functions obtained using inverse-analysis methodologies provide a means to estimate the dielectric response characteristics. The calculated absorbance functions do not necessarily converge to zero at the spectral measurement

Manuscript approved May 20, 2022.

limits. Therefore, the spectral behavior at the wavelength limits may influence the Kramers-Kronig integration and in-turn the dielectric response functions.

The next section describes the formulation of the Kramers-Kronig analysis, which is for the estimation of dielectric responses using diffuse reflectance from materials on substrates.

3. Kramers-Kronig Analysis of Diffuse Reflectance Spectra

The Kramers-Kronig analysis provides an estimation of dielectric responses using diffuse reflectance from materials on substrates and their absorption functions obtained using inverse-analysis. For this analysis, normalized extinction functions $\langle \alpha_N(\lambda) \rangle$ are determined by inverse spectral analysis of diffuse-reflectance spectra using the Kubelka-Munk model, i.e.

$$\langle \alpha_N(\lambda) \rangle = \frac{f_{KM}(\lambda)}{\max[f_{KM}(\lambda)]} \qquad (Eq.2)$$

and

$$f_{KM}(\lambda) = \frac{\left(1 - R_n(\lambda)\right)^2}{2R_n(\lambda)}, \qquad (Eq.3)$$

where R_n is the normalized reflectance relative to background, e.g., substrate. Next, a normalized imaginary index of refraction is calculated by

$$\langle k_N(\lambda) \rangle = \frac{\langle k(\lambda) \rangle}{\max[k(\lambda)]}, \qquad (Eq.4)$$

where

$$\langle k(\lambda) \rangle = \frac{\langle \alpha_N(\lambda) \rangle \lambda}{4\pi}, \qquad (Eq.5)$$

and a normalized real-refractive-index change is calculated by the Kramers-Kronig relation,

$$\langle \Delta n_N(\lambda) \rangle = \frac{2\lambda^2}{\pi} P \int_0^\infty \frac{\langle k_N(z) \rangle dz}{z(\lambda^2 - z^2)}. \qquad (Eq.6)$$

The normalization procedures defined in Eqs.(2) and (4), are consistent with the Kubelka-Munk model of diffuse reflectance, with

$$f_{KM}(\lambda) = \frac{C_{abs}}{C_{scat}}, \qquad (Eq.7)$$

where C_{abs} and C_{scat} are the absorption and scattering coefficients, respectively. Adopting the approximation of a scattering coefficient C_{scat} as being weakly dependent on wavelength, it follows that

$$\langle \alpha_N(\lambda) \rangle \propto C_{abs}. \qquad (Eq.8)$$

Therefore, a multiplicative factor approximates the dependence on scatterer density. Additionally, the Kubelka-Munk function in Eq. (2) is inherently an approximation of the absorbance function.

Further, we assume that the wavelength integration range of Eq. (6) is incomplete, but of sufficient expanse for estimating real-refractive-index change. Sensitivity with respect to incompleteness of the wavelength range of integration can be quantified by extrapolation procedures at the limits of the measured spectral range.

Continuing the analysis procedure, a scaling parameter C_s represents the dependence on scatterer density, defined by

$$\alpha_s(\lambda) = C_s\langle\alpha_N(\lambda)\rangle. \quad (Eq.9)$$

Accordingly, the dependence of the complex index of refraction on scatterer density is

$$k_s(\lambda) = C_s\langle k_N(\lambda)\rangle \quad (Eq.10)$$

and

$$n_s(\lambda) = 1 + C_s\langle\Delta n_N(\lambda)\rangle. \quad (Eq.11)$$

The estimated complex dielectric-response function is then

$$\langle\varepsilon(\lambda, C_s)\rangle = \langle\varepsilon_r(\lambda, C_s)\rangle + i\langle\varepsilon_i(\lambda, C_s)\rangle, \quad (Eq.\ 12)$$

where

$$\langle\varepsilon_r(\lambda, C_s)\rangle = \big(n_s(\lambda)\big)^2 - \big(k_s(\lambda)\big)^2 \quad (Eq.13)$$

and

$$\langle\varepsilon_i(\lambda, C_s)\rangle = 2\, n_s(\lambda)\, k_s(\lambda). \quad (Eq.14)$$

Numerical integration of Eq. (6) for this analysis uses the discrete Kramers-Kronig relation

$$\Delta n_N(n) = \frac{2\lambda(n)^2}{\pi}\sum_{m=1}^{N}\frac{[(k_N(m)/\lambda(m) - (k_N(n)/\lambda(n))]}{(\lambda(n)^2 - \lambda(m)^2)}, \quad (Eq.15)$$

where $m \neq n$, ($m, n = 1, ..., N$) and $\lambda(1) = \lambda_1$, $\lambda(N) = \lambda_N$ bound the spectral region of integration.

Figures (1) presents a description of the analysis procedure defined above. The procedure as described in Fig. (1) is applied to an incomplete wavelength integration range for the measured reflectance spectra, which for some measured spectra may include noise artifacts. Accordingly, extrapolation and smoothing techniques should be applied for determining sensitivity of calculated dielectric response to integration-range incompleteness and noise filtering.

4. Case-Study Analyses

The complex index of refraction for 13 COTS dyes were estimated and evaluated using Kramers-Kronig analysis. The results from the Kramers-Kronig analysis establish fundamental material properties that can support the characterization of the dielectric response functions. The intermediate index of refraction properties are of particular interest, as they can be scaled – based on the scatterer density – to effectively estimate these dielectric response functions.

The dyes chosen for analysis have maximum-absorption wavelengths in either the NIR or SWIR bands, with appreciable spectral features extending into the visible spectrum. Reference 13 describes the procedures used for dye and dyed-fabric sample preparation, and reflectance-

spectrum measurements of dyed fabric samples. For this study, these dyes are designated according to their maximum absorption wavelengths, using the designation "KM-Maximum-Absorption-Wavelength," similar to references 14 and 15, where chemical formulae for these dyes are given.

For the index of refraction calculations, the absorption spectra input is incomplete in the sense that it does not necessarily reach zero at the lower and upper wavelengths, and it only includes a fixed bandwidth, spanning wavelengths of 350-2500 nm. This incompleteness can impact the Kramers-Kronig integration results, influencing the spectral behavior of the complex index of refraction. In order to minimize any response degradation, lower and upper wavelength smoothing, extrapolation, and termination techniques were analyzed – both for sensitivity and accuracy. The results for the 13 dyes are included below, and comprise at least three different modified extrapolation procedures per dye for comparison. For each of these results, the absorption spectra was calculated from diffuse reflectance measurements using the normalized Kubelka-Munk inverse analysis method.

KM 720

The absorption spectra for Dye KM 720 – implying an absorption peak near 720 nm – is shown in Figure 1. This spectrum reveals incomplete absorption characteristics for the lower wavelengths and an extended tail near zero for the upper wavelengths.

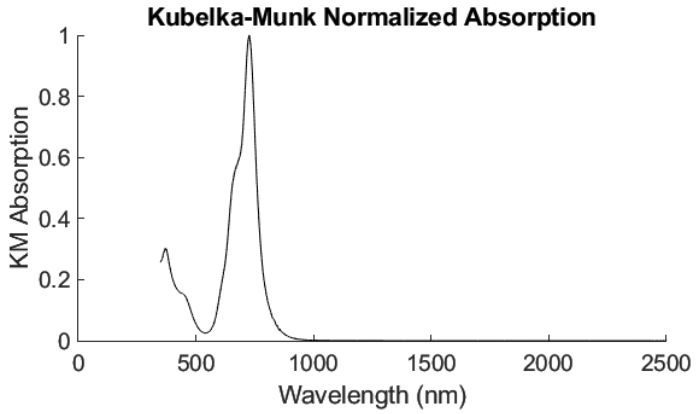

Figure 1: KM Normalized Absorption for KM 720 – calculated from diffuse reflectance measurements.

Extrapolation techniques – both at the lower and upper wavelengths – and smoothing functions were integrated to complete the region of integration and to reduce noise contributions. Different extrapolation parameters were compared to capture the sensitivity of the Kramers-Kronig analysis relative to these modifications.

The first case considered a lower wavelength extrapolation to zero with a slope of 0.0026, which aligns with the absorption behavior at the lower wavelength limit. The addition of this extrapolation did not notably impact the Kramers-Kronig index of refraction calculations, as shown in Figure 2. This is due to the extrapolation aligning closely with the spectral characteristics near 350 nm (i.e the slope is already descending towards zero).

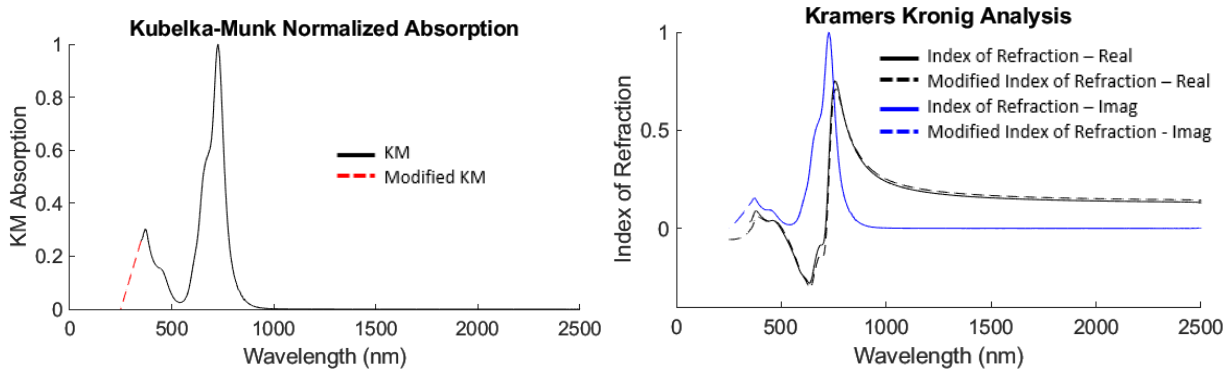

Figure 2: Case 1 - KM-720 absorption with lower wavelength extrapolation (slope: 0.0026, spanning 100 wavelengths) has minimal impact on the Kramers-Kronig Index of Refraction over the region of integration.

Upper wavelength smoothing and termination were evaluated to reduce the integration range to only span wavelengths with significant information. An example of this technique is shown in Figure 3, and also includes the lower wavelength extrapolation prior. In this case, the absorption spectrum is smoothed and terminated at zero using a 100 nm smoothing tail, starting at 1,000 nm and terminating at 1,100 nm.

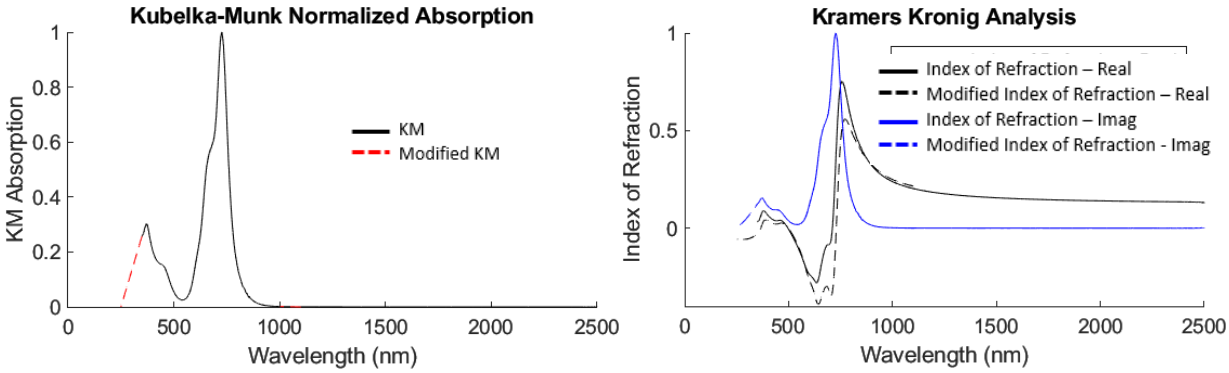

Figure 3: Case 2 - KM-720 absorption with lower wavelength extrapolation (slope: 0.0026) and higher wavelength smoothing and termination at zero at 1,100 nm (length 100).

The addition of the smoothing, termination results in lower maximums and minimums for the real index of refraction. The imaginary index of refraction is not notably impacted. This is due to the real part having a higher order dependency on the Kramers-Kronig integration. Therefore, changes at the upper (or lower) wavelengths will have a greater impact over the region of integration for the real response. If the lower wavelength extrapolation is instead extended with a reduced slope of 0.00086 (spanning 300 nm) instead of 0.0026 (spanning 100 nm), this results in greater deviations between the original and modified (post-extrapolation) indices of refraction. This is shown in Figure 4.

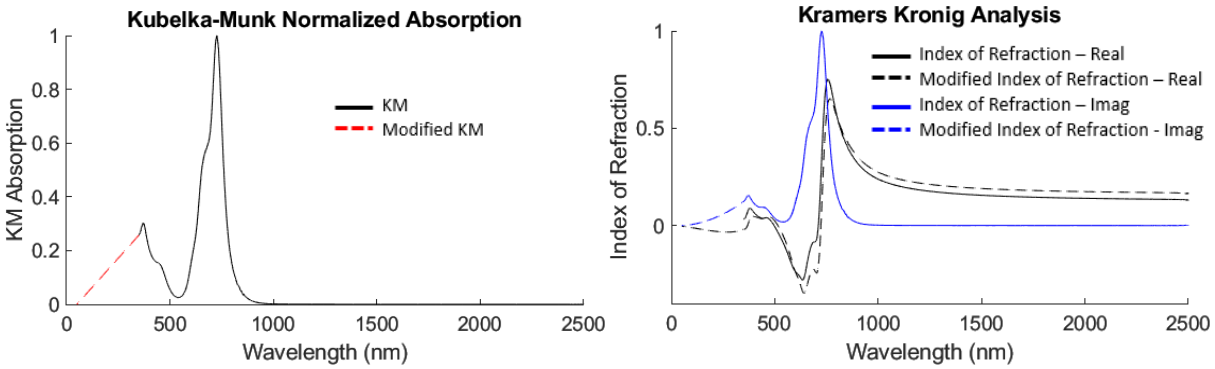

Figure 4: Case 3 - KM-720 absorption with lower wavelength extrapolation (slope: 0.00086) results in differences between the original and modified Indices of Refraction.

The smaller slope on the lower wavelength extrapolation results in slight broadening of the real index of refraction. This results from the extrapolation diverging from the original spectral characteristics at the lower wavelengths. For comparison a sharp slope (near infinite) is also considered in Figure 5.

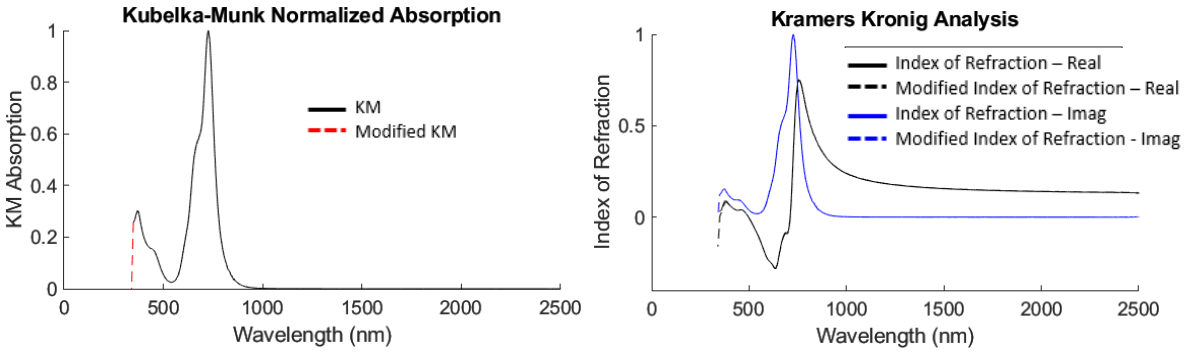

Figure 5: Case 4 - KM-720 absorption with lower wavelength extrapolation (slope: ~∞) results in minimal differences between the original and modified Indices of Refraction.

The Kramers-Kronig integration with a near vertical slope is nearly identical to the results with no extrapolation. This indicates that the incomplete integration range may cause differences in the index of refraction calculations if the missing wavelengths vary notably from the behavior near 350 nm. If the spectra continue a similar behavior and is approaching zero, minimal differences between the original and modified data are expected. For spectra's that are not nearing zero at 350 nm, effective extrapolation becomes more important in capturing accurate indices of refraction matching the lower wavelength behavior. For KM-720, the extrapolation for Case 2 is recommended, as it provides a more realistic representation of the spectra over the larger integration range and reduces higher wavelength noise with early smoothing and termination.

KM 775

A similar analysis was performed for dye KM 775, with an absorption peak near 775 nm. The calculated KM absorption spectra is approaching zero at the starting wavelength of 350 nm, so adding a lower wavelength extrapolation to zero – continuing with the same slope – has no impact on the Kramers-Kronig analysis. This is shown in Figure 6.

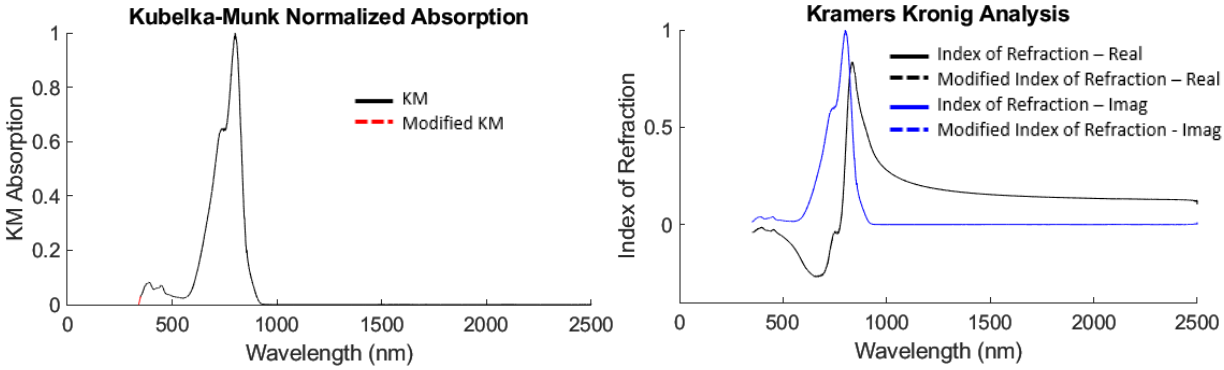

Figure 6: Case 1 – KM 775 absorption with lower wavelength extrapolation (slope: 0.0029) results in no notable difference between the original and modified Indices of Refraction.

Additionally, adding a smoothing termination at 1,000 nm results in slight shift in the estimated real index of refraction – similar to KM 720. This is shown in Figure 7.

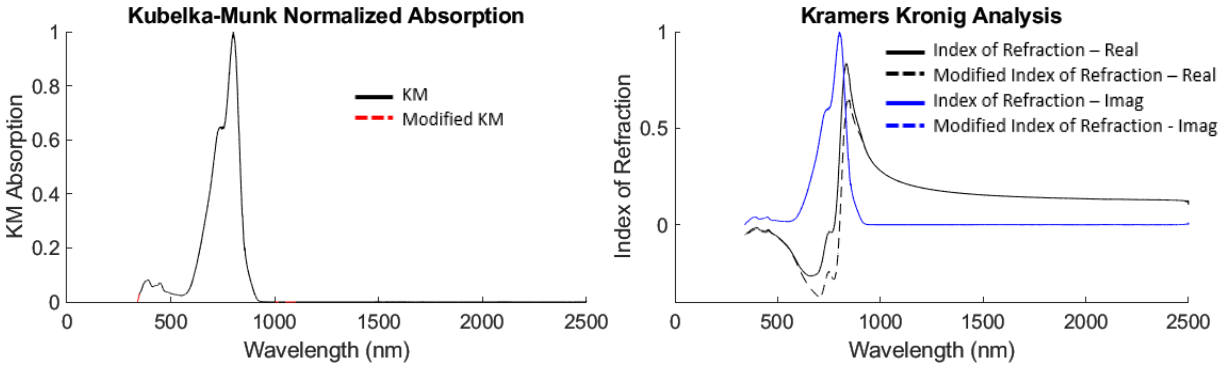

Figure 7: Case 2 – KM 775 absorption with lower wavelength extrapolation (slope: 0.0029) and upper wavelength smoothing and termination starting at 1,000 nm (length 100 nm).

Extending this smoothing termination to 1,100 nm (length 100 nm) is shown for comparison in Figure 8.

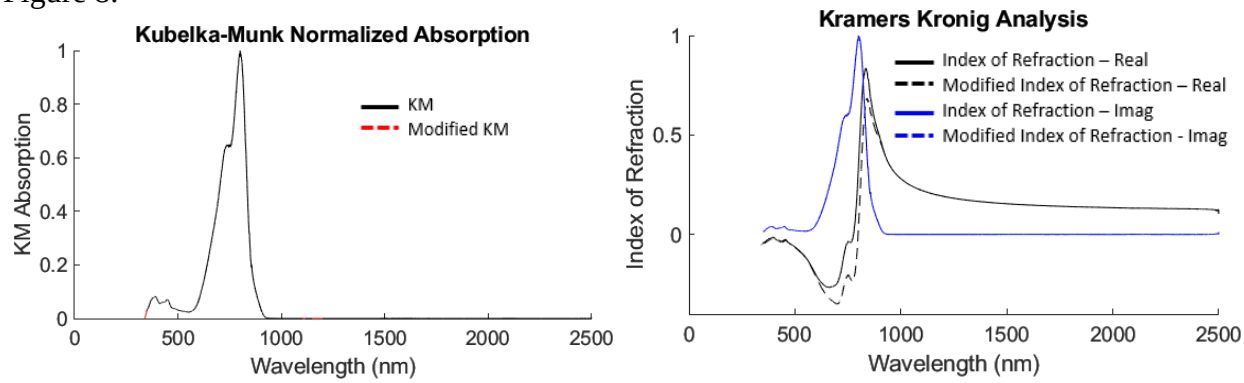

Figure 8: Case 3 – KM 775 absorption with lower wavelength extrapolation (slope: 0.0029) and upper wavelength smoothing and termination starting at 1,100 nm (length 100 nm).

The extension of this termination to higher wavelengths, shifts the real index of refraction up, closer to the original spectra. As the termination point continues to shift towards the original

spectral ending point of 2,500 nm, the curve will continue to shift up towards the original real index of refraction. For KM 775, Case 2 is recommended, as it provides smoothing and termination at higher wavelengths, reducing trailing noise, while still aligning closely with the dye's spectral behavior.

KM 778

For dye KM 778, with an absorption peak near 778 nm, the calculated KM absorption spectra is near zero at the starting wavelength of 350 nm. A short lower wavelength extrapolation – continuing with the same slope – was added to terminate the lower wavelength at zero. This has no impact on the Kramers-Kronig analysis, as shown in Figure 9.

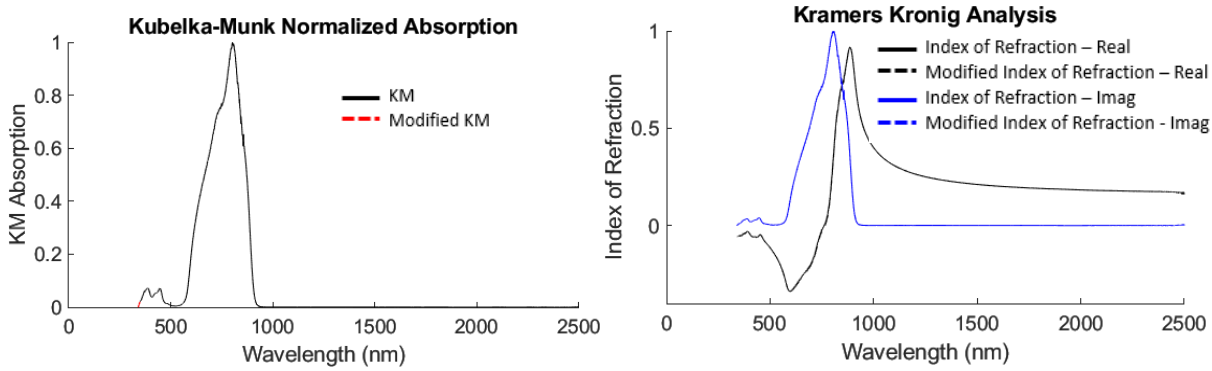

Figure 9: Case 1 – KM 778 absorption with lower wavelength extrapolation (slope: 0.0023).

The second extrapolation case considered included the previous lower wavelength extrapolation, in addition to an upper wavelength extrapolation starting at 1,000 nm and reaching zero at 1,100 nm. This extrapolation shifted the real index of refraction lower, as shown in Figure 10.

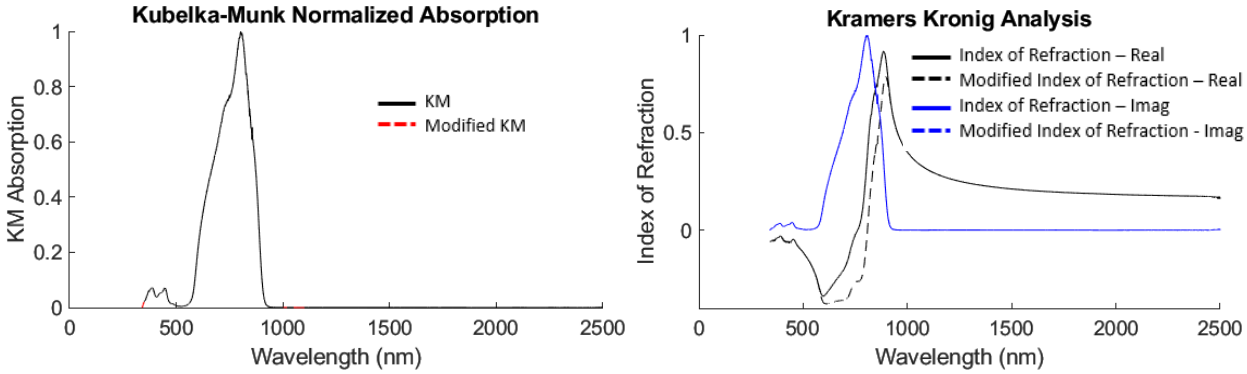

Figure 10: Case 2 – KM 778 absorption with lower wavelength extrapolation (slope: 0.0023) and upper wavelength smoothing and termination after 1,000 nm (length 100 nm).

Shortening the upper wavelength extrapolation to a length of only 50 nm, so that it terminates to zero at 1,050 nm, results in the real index of refraction shifting slightly lower, as shown in Figure 11. The more the extrapolation termination shortens the original extended tail, the more the real index of refraction peaks shift lower.

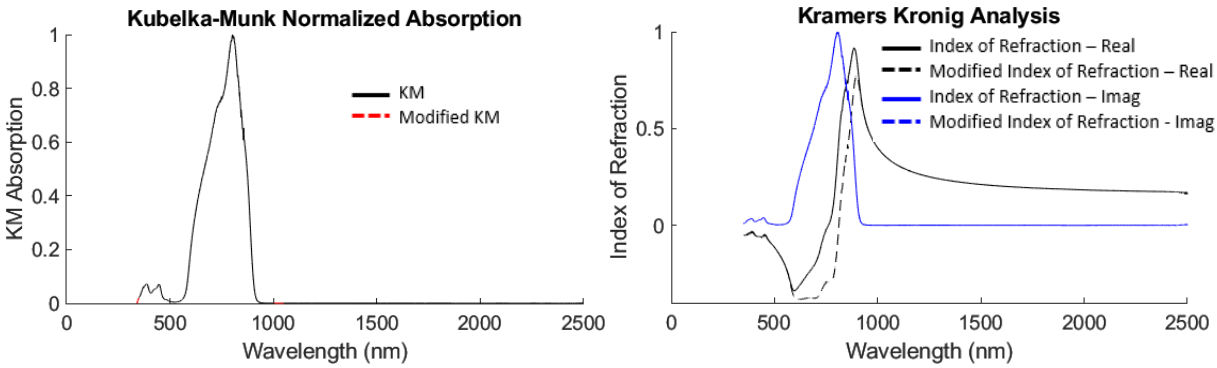

Figure 11: Case 3 – KM 778 absorption with lower wavelength extrapolation (slope: 0.0023) and upper wavelength smoothing and termination after 1,000 nm (length 50 nm).

For KM 778, Case 2 is recommended, as it provides smoothing and termination at higher wavelengths, reducing trailing noise, while also aligning closer with the dye's spectral response.

KM 780

The KM absorption for KM 780 shows a main peak near 780 nm, as well as two smaller peaks near 450 nm and 900 nm. Adding a lower wavelength extrapolation continuing with the original slope (0.0055), as shown in Figure 12, results in minimal changes to the Kramers-Kronig calculations. Additionally, a moving median filter spanning 20 nm was applied to reduce the measurement noise. This reduced the measurement spike originally located at 850 nm.

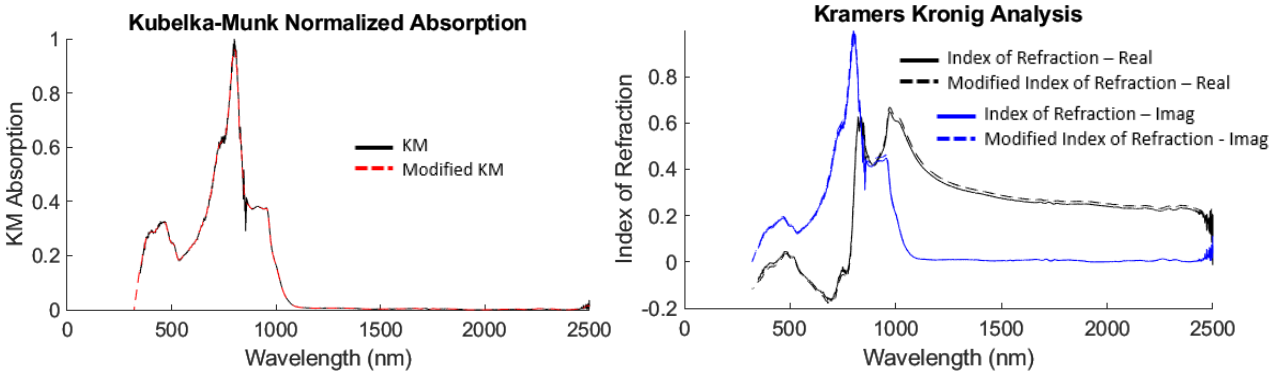

Figure 12: Case 1 – KM 780 absorption with lower wavelength extrapolation (slope: 0.0055, length 30). Also applied median smoothing filter across 20 nm.

Keeping this lower wavelength extrapolation and adding an upper wavelength termination to zero (starting at 1,500 nm and extending 100 nm), slightly modifies the real index of refraction. As shown in Figure 13, the real index of refraction shifts lower with the earlier termination. The moving median filter was also applied to this case.

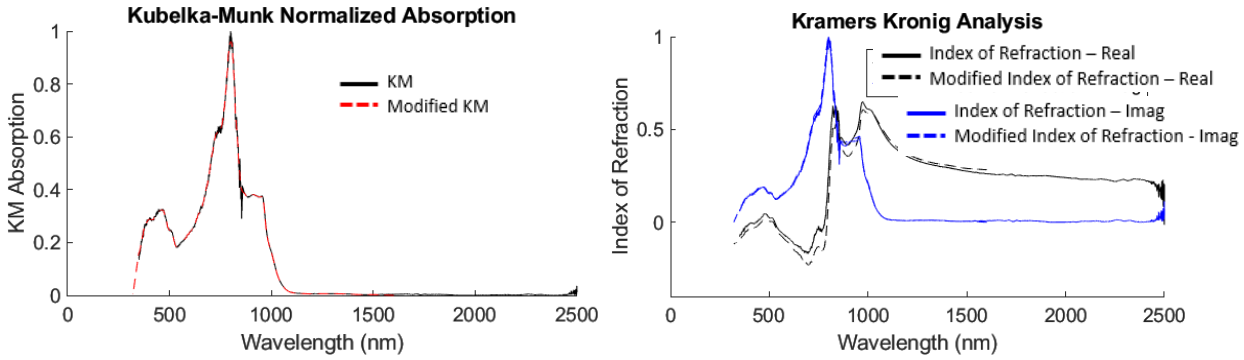

Figure 13: Case 2 – KM 780 absorption with lower wavelength extrapolation (slope: 0.0055), moving median filter spanning 20 nm, and upper wavelength smoothing and termination after 1,500 nm (length 100 nm).

For Case 3, a modified lower wavelength extrapolation was considered that broadened the lower absorption base. This slightly shifted the real index of refraction, though the differences are minimal. In this case, the moving median filter of 20 nm was also applied. These results are compared in Figure 14.

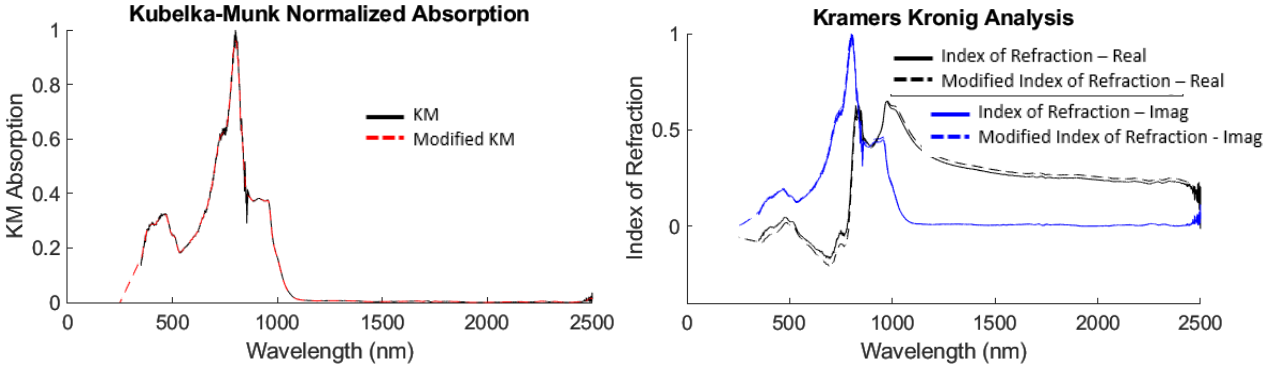

Figure 14: Case 3 – KM 780 absorption with lower wavelength extrapolation (slope: 0.0016, length 100) and moving average spanning 20 nm.

For KM 780, Case 2 is recommended for minimizing noise and capturing the spectral area of interest. Since there is minimal sensitivity to the lower wavelength extrapolation slope (as shown in Case 3), the estimated spectral behavior can be held with higher confidence.

KM 825

Dye KM 825 contains a main absorption peak near 825 nm and a much smaller absorption peak near 425 nm. Applying an extrapolation to the lower wavelengths for absorption termination results in no changes to the Kramers-Kronig index of refractions, so long as the extrapolation maintains the lower wavelength slope towards zero. This is shown in Figure 15.

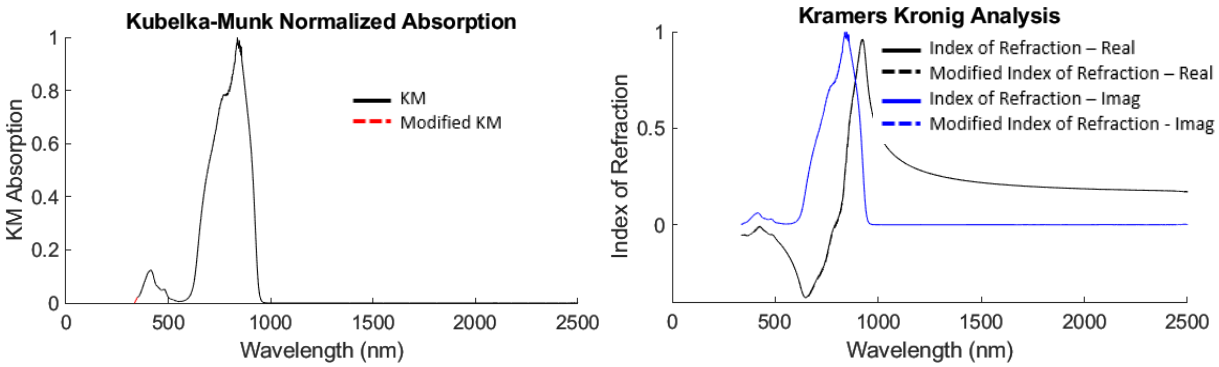

Figure 15: Case 1 – KM 825 absorption with lower wavelength extrapolation (slope: 0.0015, length 15).

Case 2 added an upper wavelength extrapolation to Case 1. The absorption curve was extrapolated at 1,000 nm to zero, spanning 100 nm. This termination, as expected, resulted in a slight decrease in the real index of refraction peaks, as shown in Figure 16.

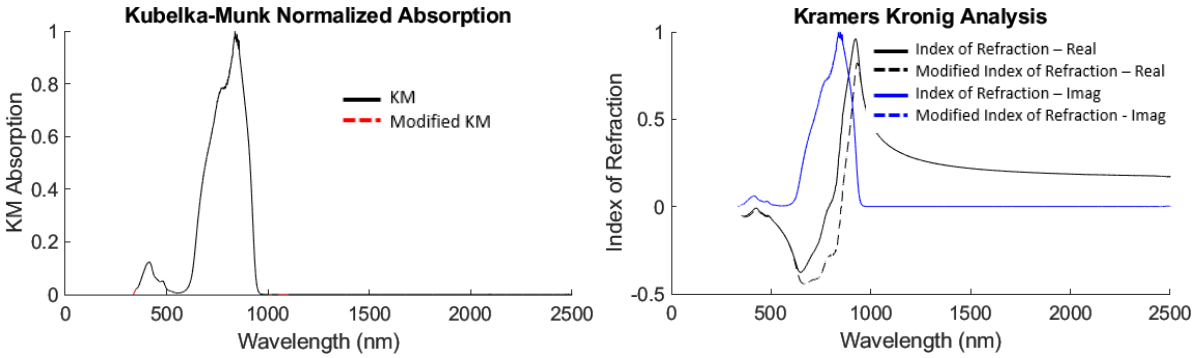

Figure 16: Case 2 – KM 825 absorption with lower wavelength extrapolation (slope: 0.0015, length 15) and upper wavelength smoothing and termination after 1,000 nm (length 100 nm).

Shortening the upper wavelength extrapolation in Case 2 to a length of only 50 nm results in a slightly lower real index of refraction response. This is shown in Figure 17.

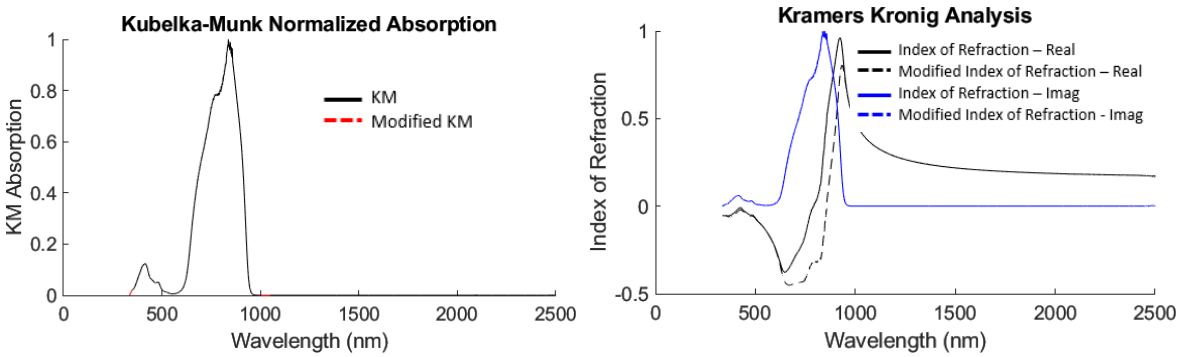

Figure 17: Case 3 – KM 825 absorption with lower wavelength extrapolation (slope: 0.0015, length 15) and upper wavelength smoothing and termination after 1,000 nm (length 50 nm).

For KM 825, Case 2 is recommended, as it provides smoothing and termination at higher wavelengths, reducing trailing noise, while still aligning closely with the dye's spectral behavior.

KM 832

Dye KM 832 has its main absorption peak near 832 nm and a secondary absorption peak near 445 nm. At the lower wavelength of 350 nm, the absorption curve approaches zero. Extending this slope towards zero with a slope of 0.005 (length of 20 nm) results in no noticeable modification in the calculated indices of refraction, as shown in Figure 18.

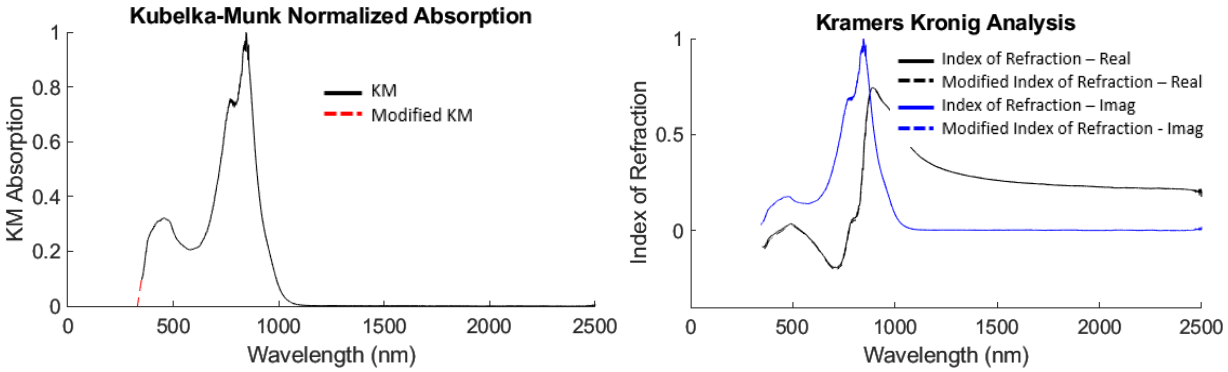

Figure 18: Case 1 – KM 832 absorption with lower wavelength extrapolation (slope: 0.005, length 20 nm).

Modifying the lower extrapolation, such that it instead consists of a wider absorption base, causes slight changes in the indices of refraction. For a lower wavelength extrapolation length of 100, slight adjustments in results of the Kramers-Kronig analysis are shown in Figure 19.

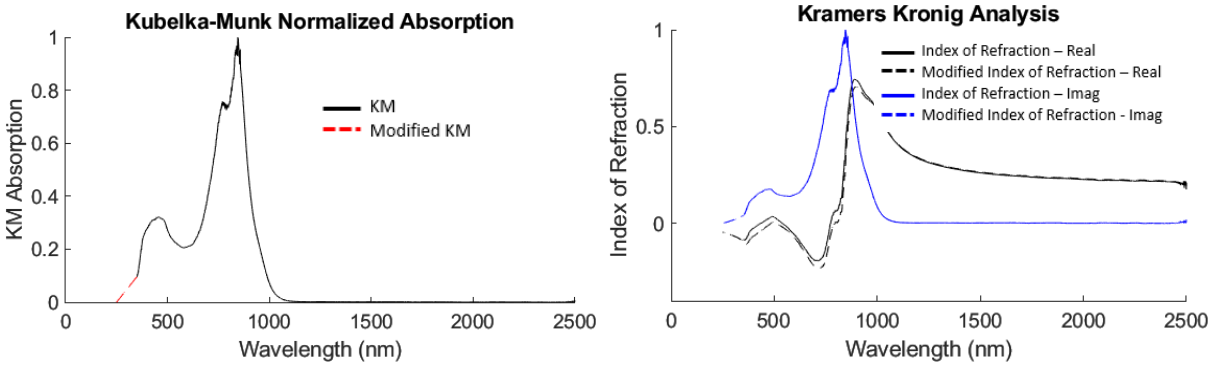

Figure 19: Case 2 – KM 832 absorption with lower wavelength extrapolation (slope: 0.00096, length 100).

Taking the lower wavelength extrapolation from Case 1, and adding an upper wavelength termination starting at 1,100 nm for a length of 100 nm, causes a notable shift down in the real index of refraction curve. This is shown in Figure 20.

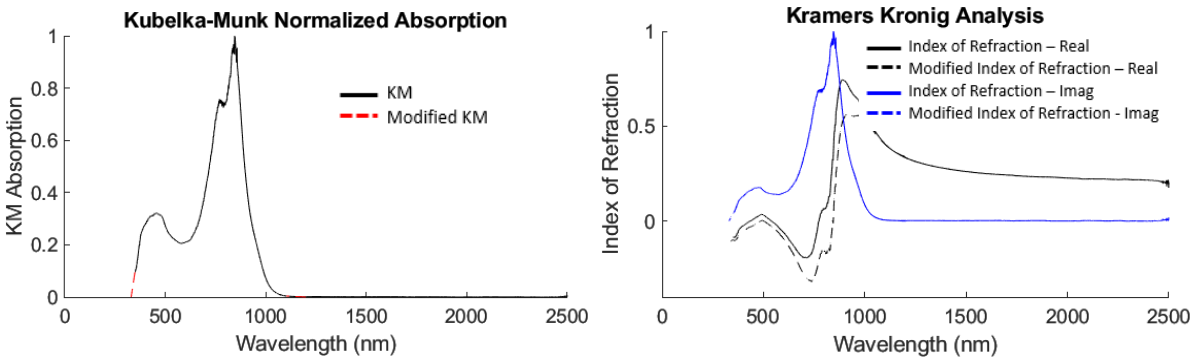

Figure 20: Case 3 – KM 832 absorption with lower wavelength extrapolation (slope: 0.005, length 20 nm) and upper wavelength termination at 1,100 nm (length 100 nm).

For KM 832, Case 3 is recommended, as it provides smoothing and termination at lower and higher wavelengths, reduces trailing noise, and still aligns closely with the dye's spectral behavior.

KM 836

Dye KM 836, with a lower wavelength extrapolation to zero (slope 0.0044) that aligns with the absorption slope at 350 nm, is shown in Figure 21. This modification results in no noticeable changes to the Kramers-Kronig calculations.

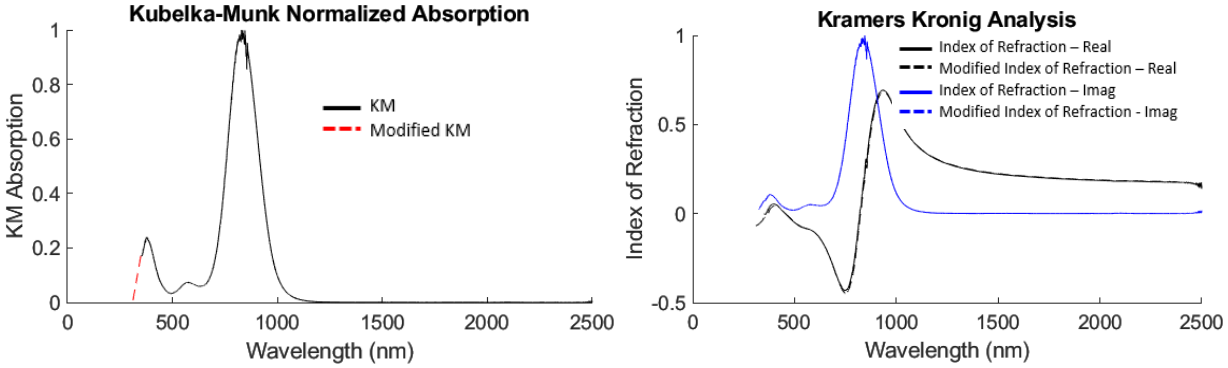

Figure 21: Case 1 – KM 836 absorption with lower wavelength extrapolation (slope: 0.0044, length 40).

Case 1 is expanded upon in Figure 22, such that it also includes a median smoothing filter spanning 20 nm. This removes the measurement noise observed near the absorption peak of 836 nm. The smoothing function causes very minimal shift in the real index of refraction, as shown in Figure 22.

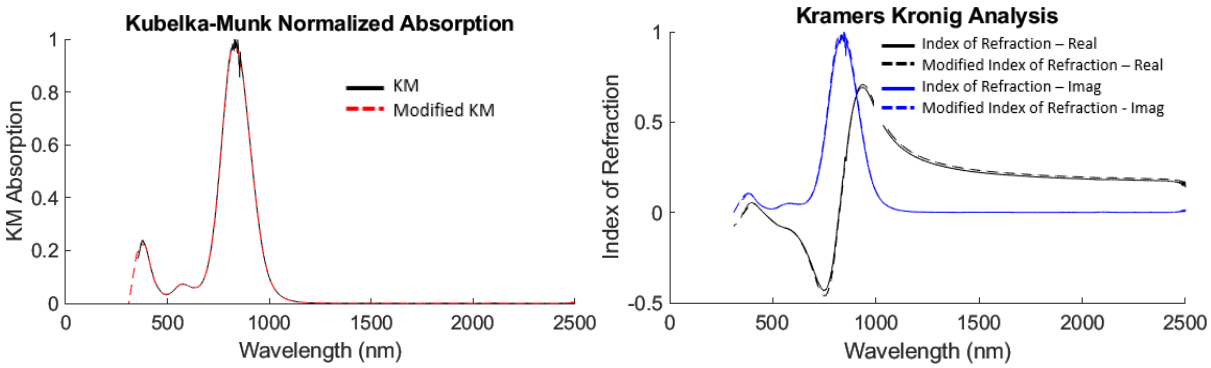

Figure 22: Case 2 – KM 836 absorption with lower wavelength extrapolation (slope: 0.0044, length 40) and a median smoothing filter of 20 nm.

Case 2 is then expanded upon in Figure 23, such that it also includes an upper wavelength termination at 1,200 nm for a length of 100 nm. This termination results in a noticeable shift lower for the index of refraction near the peak absorption wavelengths.

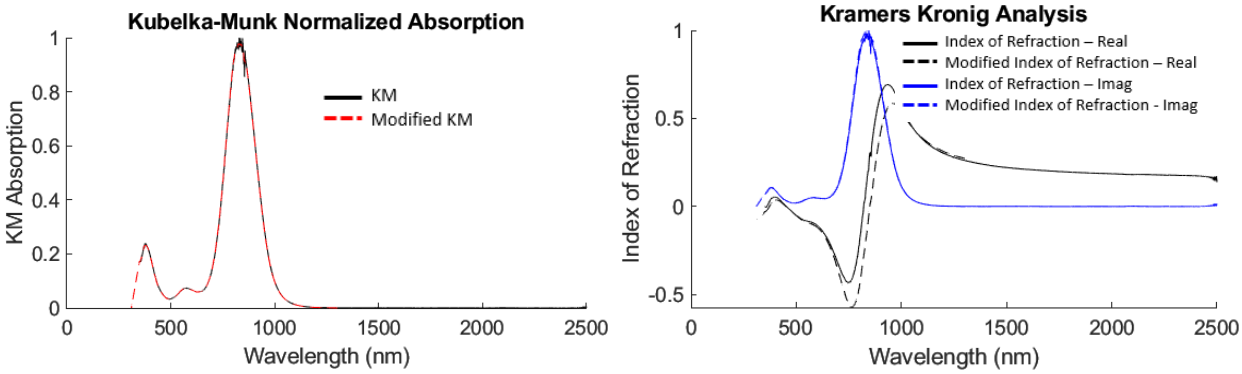

Figure 23: Case 3 – KM 836 absorption with lower wavelength extrapolation (slope: 0.0044, length 40), median smoothing filter of 20 nm, and an upper wavelength extrapolation at 1,200 (length 100 nm).

For KM 836, Case 3 is recommended, as it provides smoothing and termination at lower and higher wavelengths, reduces trailing noise, and still aligns closely with the dye's spectral behavior.

KM 845

Dye KM 845 has two absorption peaks, its main absorption peak near 845 nm and a secondary absorption peak near 374 nm. The lower wavelength termination of the secondary peak is incomplete within the measurement range. Adding a lower extrapolation with a slope 0.0052 (length 50) and applying a median smoothing filter (length 20 nm) does not change the indices of refraction noticeably. This is shown in Figure 24.

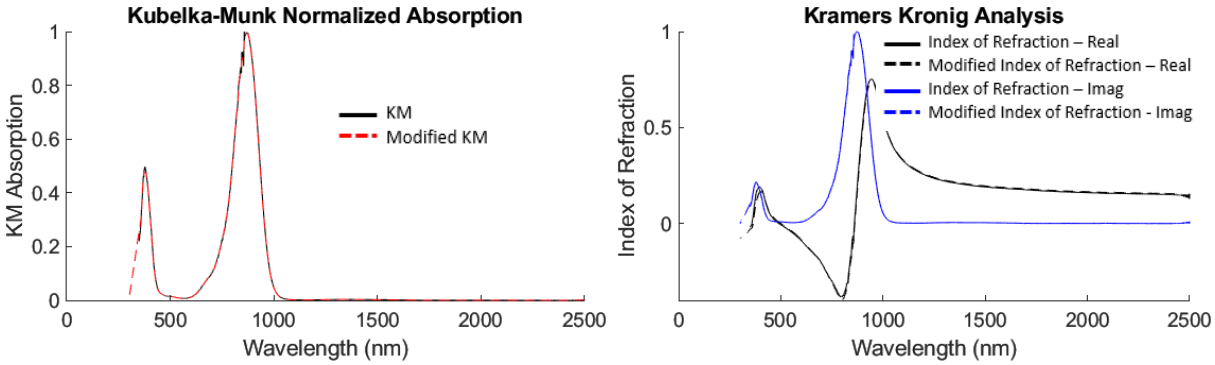

Figure 24: Case 1 – KM 845 absorption with lower wavelength extrapolation (slope: 0.0052, length 50) and median smoothing filter of 20 nm.

Doubling the length of the lower extrapolation to 100 (slope 0.026) results in the KM absorption shown in Figure 25. This modification still does not change the Kramers-Kronig analysis significantly from the original associated with an incomplete wavelength integration range.

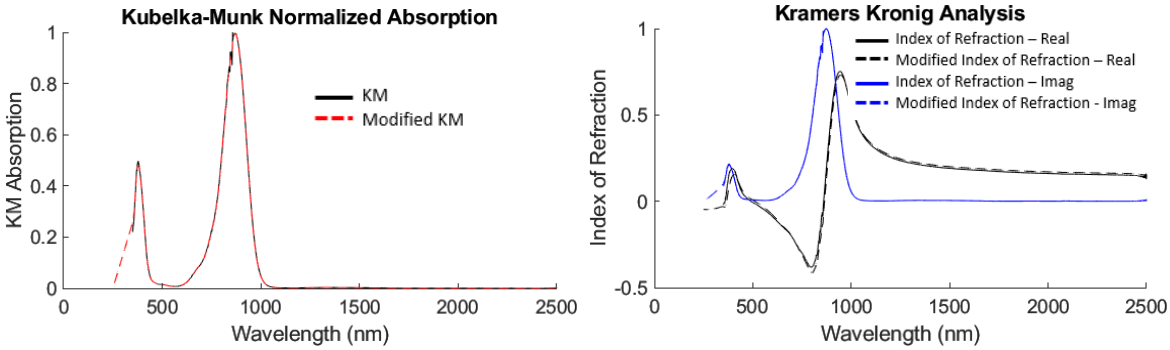

Figure 25: Case 2 – KM 845 absorption with lower wavelength extrapolation (slope: 0.026, length 100) and median smoothing filter of 20 nm.

Using the first case, with a lower wavelength extrapolation of 50 nm, and adding an upper wavelength extrapolation at 1,100 nm (length 100 nm), results in the indices of refraction shown in Figure 26. This addition of an upper wavelength termination lowers the real indices of refraction peaks.

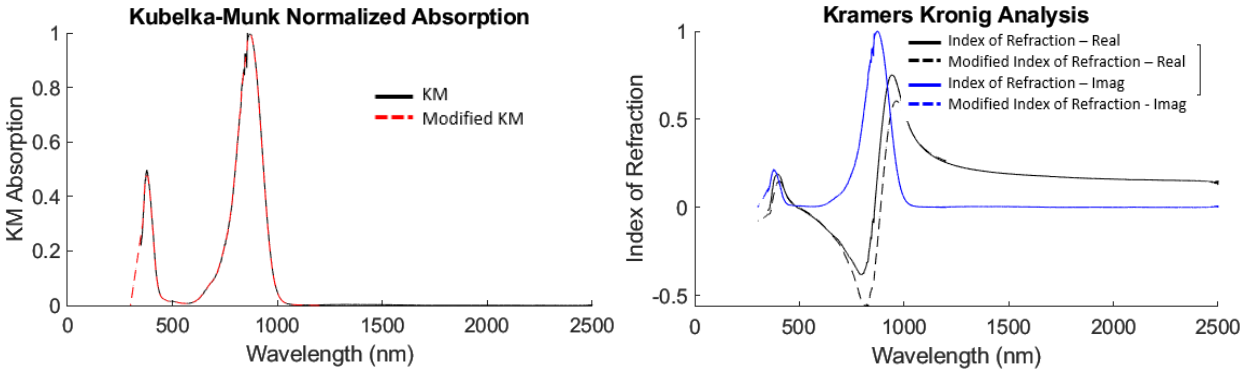

Figure 26: Case 3 – KM 845 absorption with lower wavelength extrapolation (slope: 0.0052, length 50), median smoothing filter of 20 nm, and lower wavelength termination at 1,100 nm (length 100 nm).

For KM 845, Case 2 is recommended, as it provides smoothing and termination at lower and higher wavelengths, reduces trailing noise, and aligns closer to the dye's spectral behavior.

KM 848

Dye KM 848 is very similar to Dye KM 845, with its absorption peak slightly shifted to a higher wavelength. Following the analysis for Dye KM 845, a similar lower wavelength extrapolation with a slope of 0.005 (length 50) was applied to terminate the secondary absorption peak at zero. Similar to KM 845 this had a negligible impact on the indices of refraction, as shown in Figure 27.

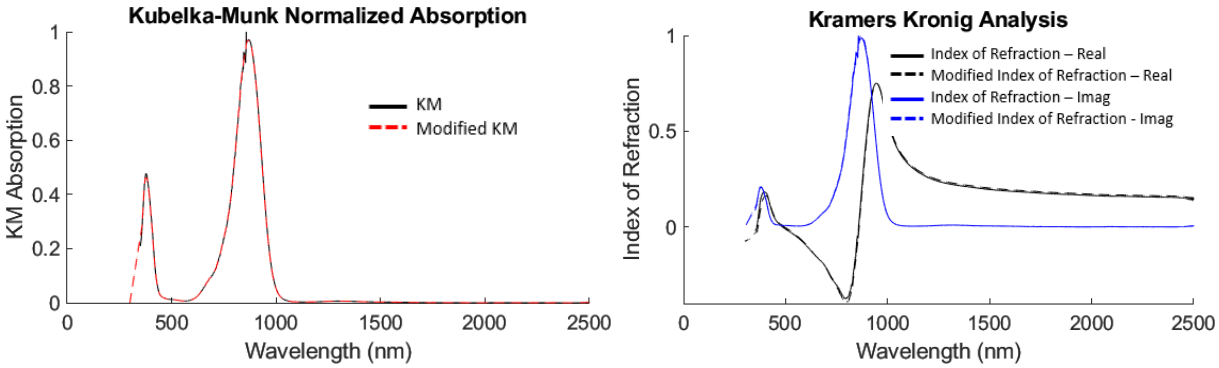

Figure 27: Case 1 – KM 848 absorption with lower wavelength extrapolation (slope: 0.005, length 50) and median smoothing filter of 20 nm.

Similar to Dye KM 845, an upper wavelength termination at 1,100 nm (length 100 nm) was applied. This resulted in a similar down shift for the real index of refraction, as shown in Figure 28.

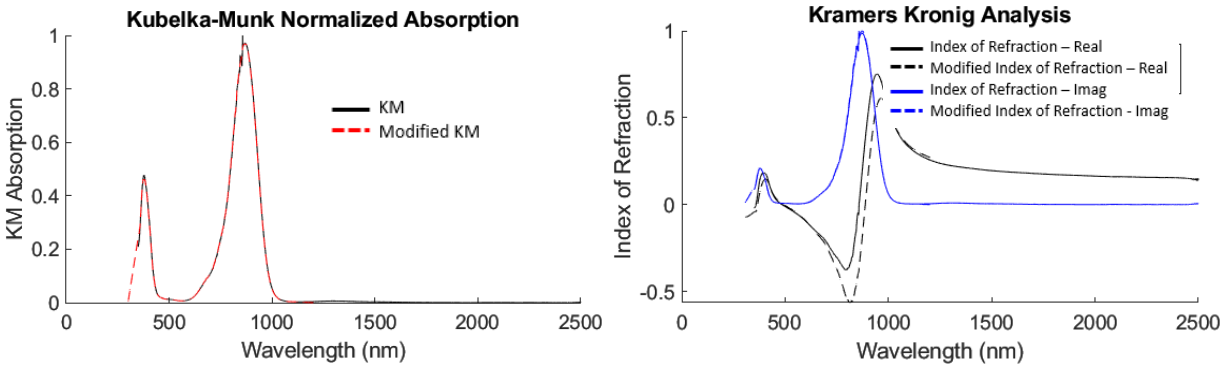

Figure 28: Case 2 – KM 848 absorption with lower wavelength extrapolation (slope: 0.005, length 50), median smoothing filter of 20 nm, and lower wavelength termination at 1,100 nm (length 100 nm).

For Case 3, the lower extrapolation was shortened to a length of 50 nm, as shown in Figure 29.

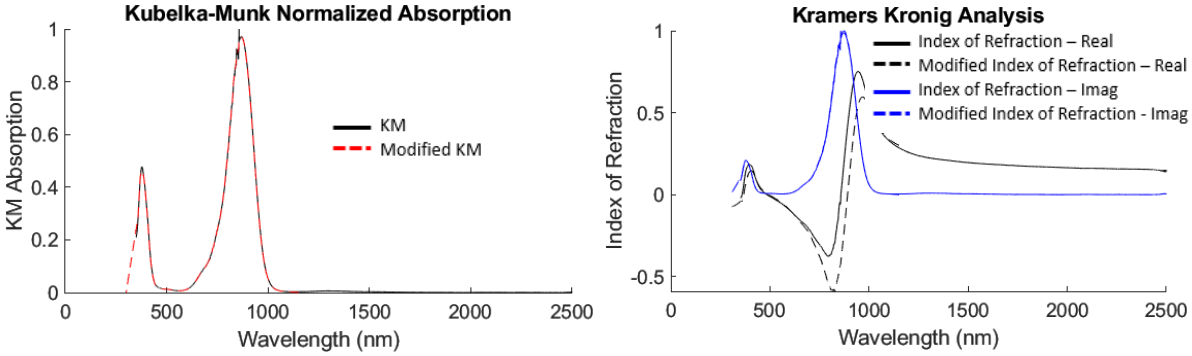

Figure 29: Case 3 – KM 848 absorption with lower wavelength extrapolation (slope: 0.005, length 50), median smoothing filter of 20, and lower wavelength termination at 1,100 nm (length 50 nm).

In this case the real index of refraction does not change noticeably, as the change in termination length is minimal. For KM 848, the smoothing and termination in Case 2 is recommended for closing the integration range.

KM 920

Dye KM 920's measurement included measurement noise in the primary peak near 900 nm. The measurement range also cut off the secondary peaks at lower wavelengths. To address these issues, a lower wavelength extrapolation was applied with a slope matching the original absorption curve (slope 0.011, length 30 nm). Additionally, a moving median smoothing filter (length 20 nm) was applied to reduce the measurement noise. The resulting absorption and results of Kramers-Kronig analysis are shown in Figure 30.

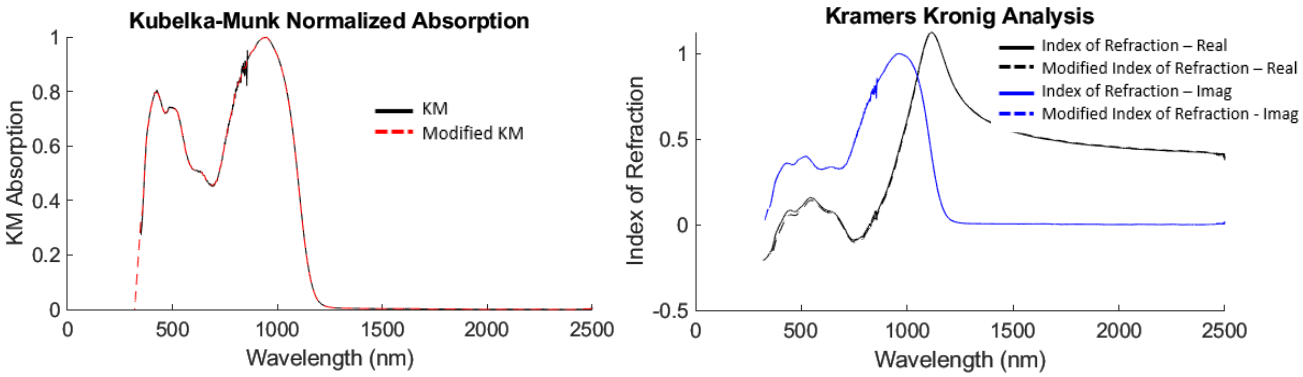

Figure 30: Case 1 – KM 920 absorption with lower wavelength extrapolation (slope: 0.011, length 30 nm) and median smoothing filter of 20 nm.

Next, extending the lower wavelength extrapolation in Case 1 to a length of 150 nm, causes a slight deviation in the real index of refraction. This is shown in Figure 31.

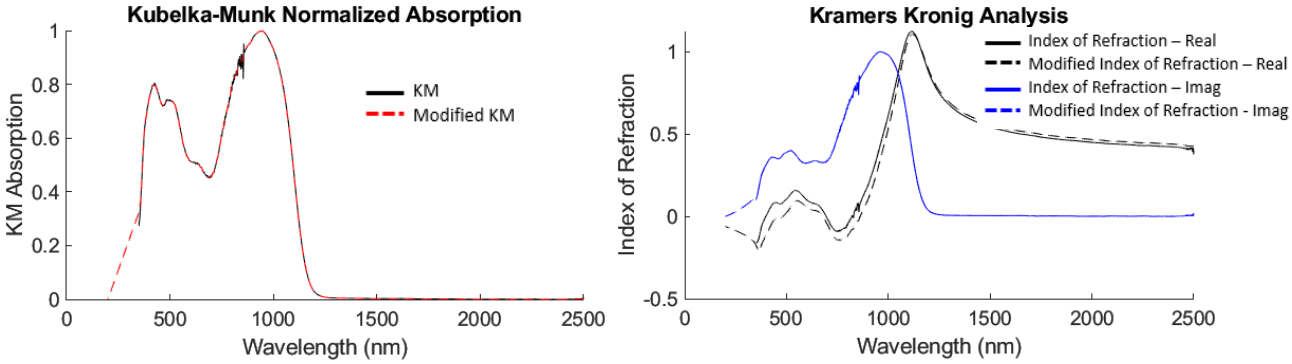

Figure 31: Case 2 – KM 920 absorption with lower wavelength extrapolation (slope: 0.011, length 150 nm) and median smoothing filter of 20 nm.

Returning to Case 1, with the lower extrapolation length of 30 nm, and adding an upper termination point at 1,400 nm (length 100 nm), results in a larger shift down in the real index of refraction for the wavelengths below its peak at 1,120 nm. This change is shown in Figure 32.

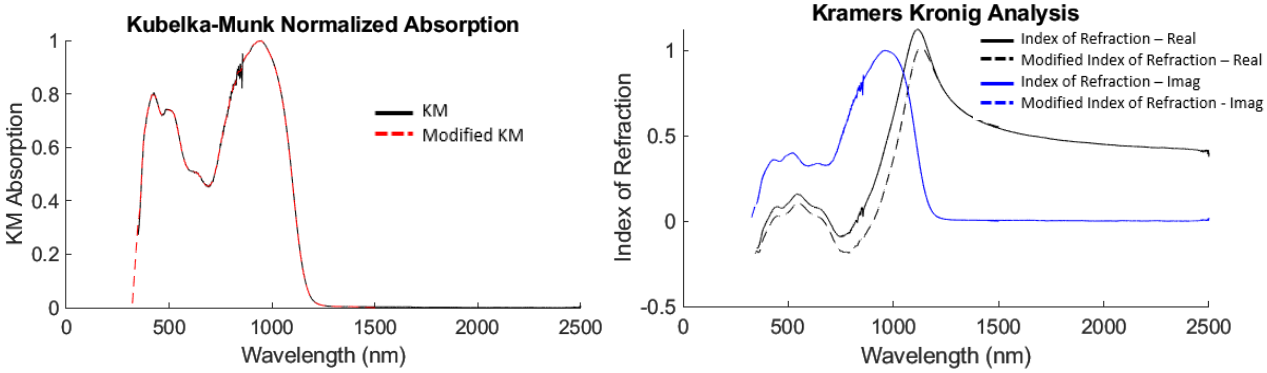

Figure 32: Case 3 – KM 920 absorption with lower wavelength extrapolation (slope: 0.0022, length 150 nm), median smoothing filter of 20 nm, and upper wavelength termination at 1,400 nm (length 100 nm).

For KM 920, Case 3 is recommended, as it provides smoothing and termination at lower and higher wavelengths, reduces trailing noise, and still aligns closely with the dye's spectral behavior.

KM 949

Dye KM 949 has measurement noise near 800 nm. A moving median smoothing filter, with a length of 20 nm, was applied to reduce this noise. Additionally, a lower wavelength extrapolation was integrated, which matches the slope at 350 nm (slope: 0.0053). These modifications are shown in Figure 33, and resulted in a smoother Kramers-Kronig result.

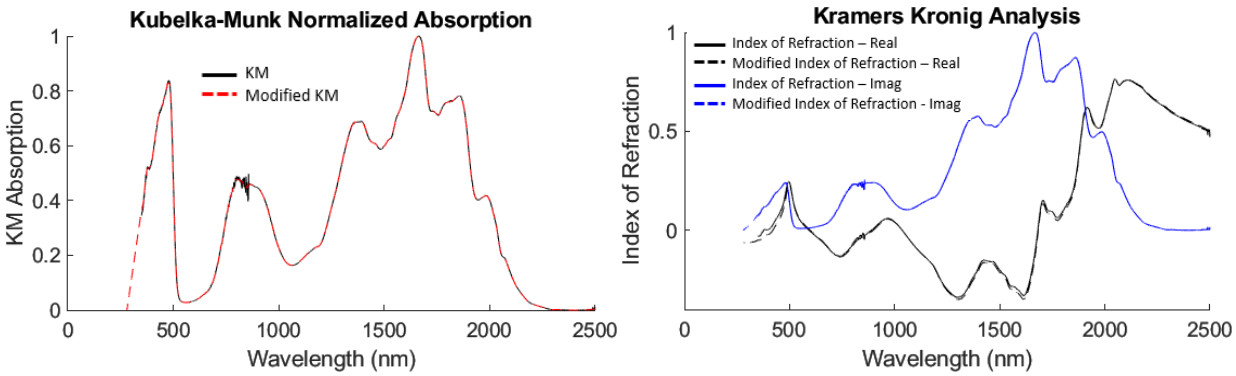

Figure 33: Case 1 – KM 949 absorption with lower wavelength extrapolation (slope: 0.0053, length 70 nm) and median smoothing filter of 20 nm.

Next, modifying the lower wavelength extrapolation, such that the slope is only 0.0025, increases the lower wavelength absorption base and causes a slight shift in the real index of refraction. This is shown in Figure 34.

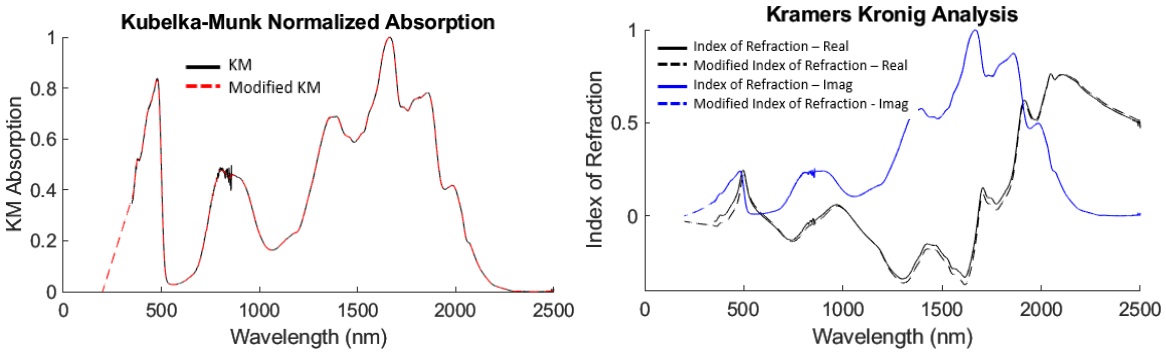

Figure 34: Case 2 – KM 949 absorption with lower wavelength extrapolation (slope: 0.0025, length 150 nm) and median smoothing filter of 20 nm.

Returning to the lower wavelength extrapolation in Case 1, keeping the median smoothing filter, and now applying an upper wavelength termination at 2,200 nm results in a slight shifting of the real index of refraction, particularly at wavelengths between 1,300-2,200 nm. This is shown in Figure 35.

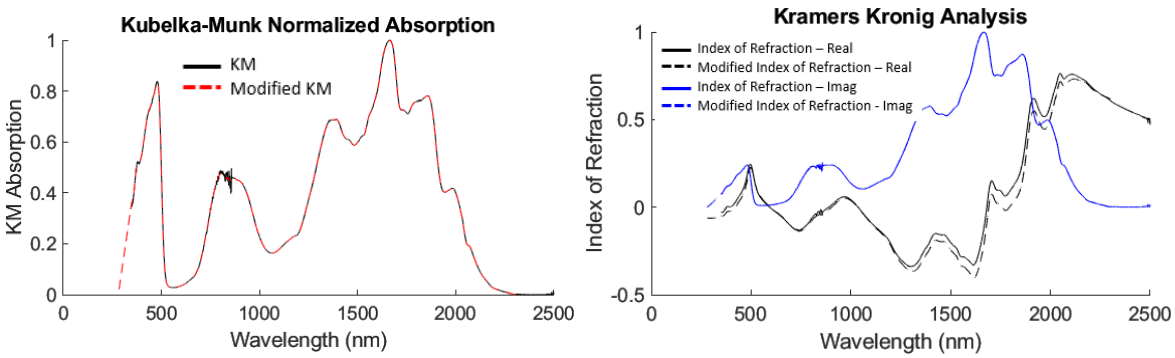

Figure 35: Case 3 – KM 949 absorption with lower wavelength extrapolation (slope: 0.0053, length 70 nm), median smoothing filter of 20 nm, and upper wavelength termination at 2,200 (length 100 nm).

For KM 949, Case 3 is recommended, as it completes the integration range, while aligning closely with the dye's spectral behavior.

KM 978

KM 978 absorption contains two peaks, a main peak at 978 nm and a secondary peak near 400 nm. Applying a lower wavelength extrapolation, matching the original slope, and smoothing the measurement noise with a median smoothing filter resulted in minimal changes to the indices of refraction (other than reducing measurement noise). This first case is shown in Figure 36.

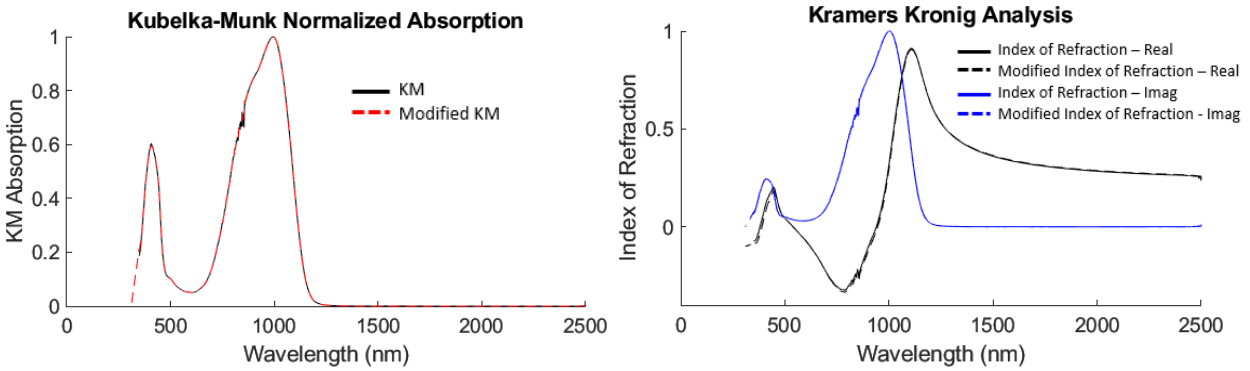

Figure 36: Case 1 – KM 978 absorption with lower wavelength extrapolation (slope: 0.0055, length 40 nm) and median smoothing filter of 20 nm.

Using the lower wavelength extrapolation in Case 1, and adding an upper wavelength termination at 1,400 nm, causes the real index of refraction peaks to shift lower, as shown in Figure 37.

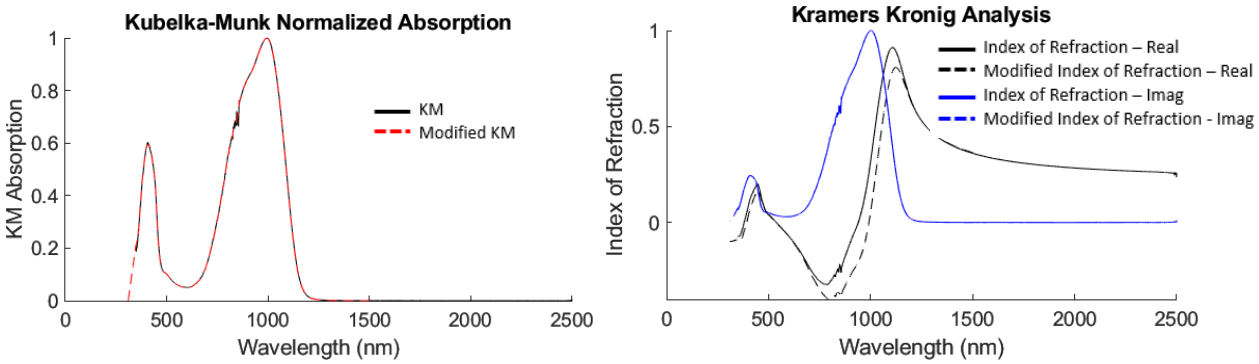

Figure 37: Case 2 – KM 978 absorption with lower wavelength extrapolation (slope: 0.0055, length 40 nm), median smoothing filter of 20 nm, and upper wavelength termination at 1,400 nm (length 100 nm).

Terminating the upper wavelengths even closer to the main absorption peak (at 1,150 nm), causes a more significant shift in the real index of refraction peaks. An example of this is shown in Figure 38.

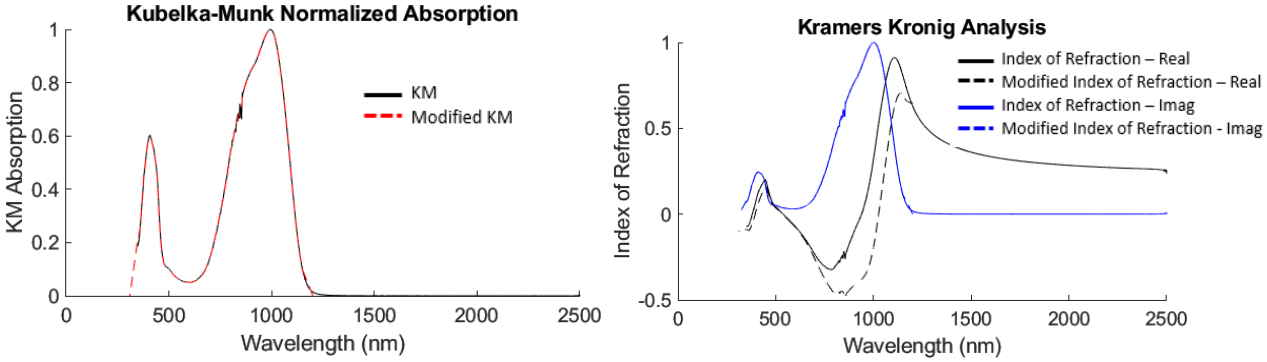

Figure 38: Case 3 – KM 978 absorption with lower wavelength extrapolation (slope: 0.0055, length 40 nm), median smoothing filter of 20 nm, and upper wavelength termination at 1,150 nm (length 50 nm).

For KM 978, Case 2 is recommended, as it provides smoothing and termination at lower and higher wavelengths, reduces trailing noise, and still aligns closely with the dye's spectral behavior.

KM 1072

A lower wavelength extrapolation was applied to KM 1072 to align with the spectral slope at the start of the measurement range. A median smoothing filter with a length of 20 nm was also applied to reduce measurement noise. As shown in Figure 39, the lower wavelength extrapolation resulted in no significant deviation in the indices of refraction.

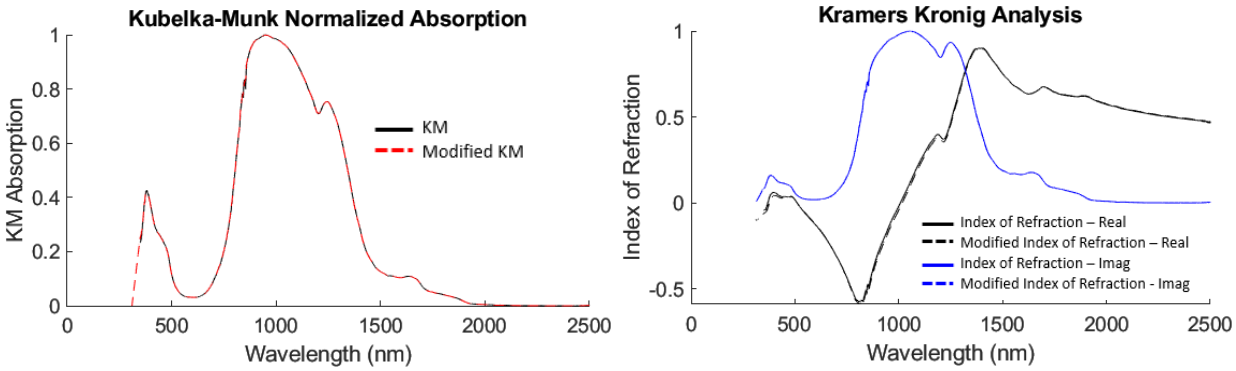

Figure 39: Case 1 – KM 1072 absorption with lower wavelength extrapolation (slope: 0.0065, length 40 nm) and median smoothing filter of 20 nm.

Building off of Case 1, and adding an upper wavelength termination starting at 2,000 nm, results in only a slight reduction in the real index of refraction peaks. This is example is shown in Figure 40.

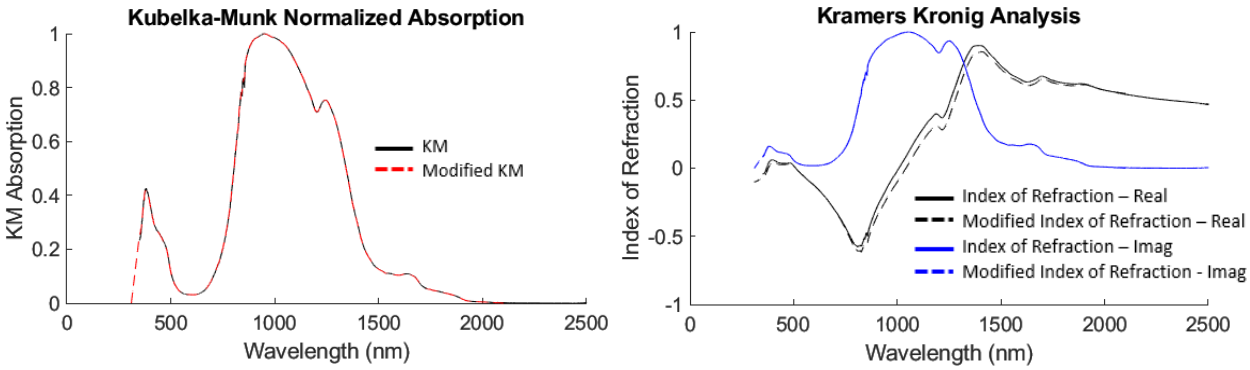

Figure 40: Case 2 – KM 1072 absorption with lower wavelength extrapolation (slope: 0.0065, length 40 nm), median smoothing filter of 20 nm, and upper wavelength termination at 2,000 nm (length 100 nm).

Starting the lower wavelength extrapolation closer to the end of the absorption peak (near 1,900 nm), causes a slightly larger shift in the real index of refraction over the center wavelengths. This case is shown in Figure 41.

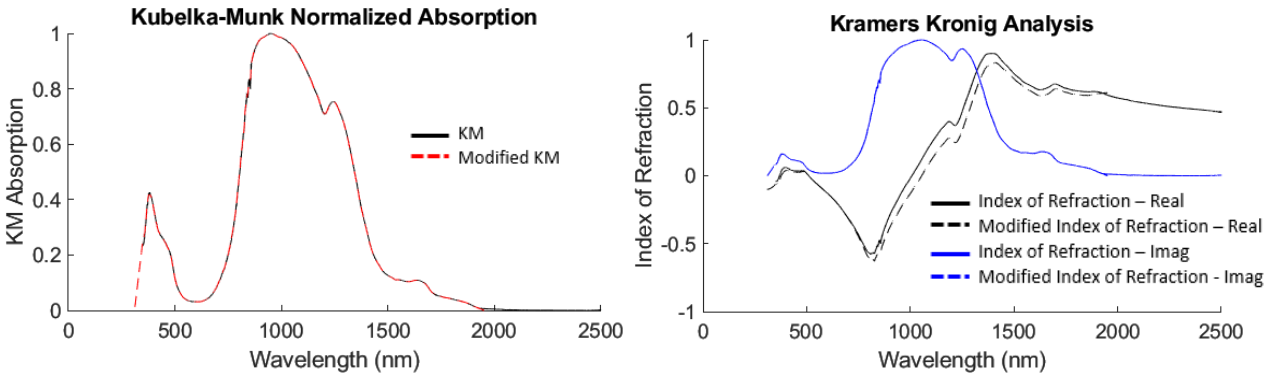

Figure 41: Case 3 – KM 1072 absorption with lower wavelength extrapolation (slope: 0.0065, length 40 nm), median smoothing filter of 20 nm, and upper wavelength termination at 1,900 nm (length 50 nm).

For KM 1072, Case 2 is recommended, as it provides smoothing and termination at lower and higher wavelengths, reduces trailing noise, and aligns closely with the dye's spectral behavior.

5. Aspects of Analysis

The extrapolation analysis provided useful insight into the Kramers-Kronig sensitivity resulting from the incomplete measurement ranges. So long as the behavior of the absorption data does not significantly change beyond the measurement range (i.e., no significant changes in slope), the estimated indices of refraction resulting from the Kramers-Kronig analysis can sufficiently represent the dye behavior.

Since lower wavelength extrapolations that align with the lower measurement range behavior do not cause notable shifts in the indices of refraction, the extrapolations are not necessary, though can be included to demonstrate completeness within the measurement range. However, the lower wavelength extrapolations are needed if the behavior is known to change at those wavelengths. The upper wavelength terminations are also recommended for dyes that have long tails near zero, as this can add additional process noise. These upper wavelength terminations should only be started after the absorption spectra has tapered off near zero.

Additionally, moving median smoothing filters are recommended for the dyes with measurement noise, as this can prevent the noise from transferring into the Kramers-Kronig analysis. Also of note, the common dye response to the extrapolation and smoothing features resulted in a slight shift (lower) of the real index of refraction. However, this shift does not significantly change the relative behavior of the index of refraction within the spectral response. Therefore, these extrapolation and smoothing procedures can provide a means to complete the integration range and minimize measurement noise, while providing more accurate representation of the dye material properties, including the indices of refraction and their associated permittivity responses.

6. Conclusion

Determining estimates of the dielectric response of NIR/SWIR-absorbing dyes poses a specific problem. This study presents and demonstrates an inverse spectral analysis procedure for determining such estimates via Kramers-Kronig analysis and KM theory. The estimated dielectric response functions can be used to construct a parametric space for developing effective-medium

models capable of estimating reflectance from dyed fabrics. Furthermore, for measurements with noise or incomplete features near the spectral limits, extrapolation/smoothing techniques can support construction of approximate effective-medium models capable of estimating reflectance from dyed fabrics.

Acknowledgement

This project was supported by U.S. DoD programs.

References

1. W.W. Wendlandt and H.G. Hecht, Reflectance Spectroscopy, John Wiley & Sons, New York (1966).
2. G. Kortum, Reflectance Spectroscopy, Springer-Verlag, Berlin (1969).
3. H.G. Hecht, "The Interpretation of Diffuse Reflectance Spectra," Journal of Research of the National Bureau of Standards-A, Physics and Chemistry, Vol. 80A, No.4, July-August (1976), pp. 567-583.
4. G. Wyszecki and W.S. Stiles, Color Science: Concepts and Methods, Quantitative Data and Formulae, 2nd ed., John Wiley &Sons, New York (1982).
5. B. Hapke, Introduction to the Theory of Reflectance and Emittance Spectroscopy, Cambridge Univ. Press, New York (1993).
6. J. Torrent and V. Barron, Diffuse Reflectance Spectroscopy, Chapter 13, Methods of Soil Analysis, Part 5, Mineralogical Methods, SSSA Book Series, no. 5, Soil Science Society of America, Madison, WI, 2008, pp. 367-385.
7. C.F. Bohren and D.R. Huffman, Absorption and Scattering of Light by Small Particles, Wiley-VCH, 2004.
8. M. Born and E. Wolf, Principles of Optics, 2nd. ed., Pergamon, London, 1964.
9. V. Dzimbeg-Malcic, Z. Barbaric-Mikocevic, K. Itric, "Kubelka-Munk Theory in Describing Optical Properties of Paper (I)," Technical Gazette 18, 1 (2011), pp.117-124.
10. P. Kubelka, F. Munk, "Ein Beitrag zur Optik der Farbanstriche," Z. Tech. Phys. (Leipzig), 12 (1931), pp. 593-601.
11. P. Kubelka, "New Contributions to the Optics of Intensely Light-Scattering Materials. Part I," J. Opt. Soc. Am., 38 (1948), pp. 448-457.
12. P. Kubelka, "New Contributions to the Optics of Intensely Light-Scattering Materials. Part II," J. Opt. Soc. Am., 44 (1954), pp. 330-335.
13. R. Viger, S. Ramsey, T. Mayo, S.G. Lambrakos, "Parametric Modeling of Reflectance Spectra for Dyes and Their Mixtures in Fabrics Using Reference Spectra," Journal of Electromagnetic Waves and Applications, Vol. 33, No. 9, pp. 1163-1171, (2019).
14. Fabricolor Holding International Product List, Laser and Fluorescent dyes, UV and NIR dyes, security inks and other optically functional materials, Code FHI 7206.
15. American Dye Source, Inc., ADS 775PI, CAS # 207399-07-3, 555 Morgan Boulevard, Baie D'Urfe, Quebec, Canada.